Earth and Planetary Science Letters 310 (2011) 192–202

Contents lists available at SciVerse ScienceDirect

Earth and Planetary Science Letters

journal homepage: www.elsevier.com/locate/epsl

Holocene tropical South American hydroclimate revealed from a decadally resolved lake sediment $\delta^{18}O$ record

Broxton W. Bird [a,*], Mark B. Abbott [a], Donald T. Rodbell [b], Mathias Vuille [c]

[a] University of Pittsburgh, Department of Geology and Planetary Science, 4107 O'Hara St., Pittsburgh, PA 15260, United States
[b] Union College, 807 Union St., Geology Department, Schenectady, NY 12308, United States
[c] University at Albany, State University of New York, Department of Earth and Atmospheric Sciences, 1400 Washington Ave, Albany, NY 12222, United States

ARTICLE INFO

Article history:
Received 5 May 2011
Received in revised form 20 August 2011
Accepted 26 August 2011
Available online xxxx

Editor: P. DeMenocal

Keywords:
South American summer monsoon
oxygen isotopes
precessional forcing
abrupt climate change
lake sediments

ABSTRACT

Oxygen isotope ratios of authigenic calcite ($\delta^{18}O_{cal}$) measured at annual to decadal resolution from Laguna Pumacocha document Andean precipitation variability during the last 11,200 years. Modern limnological data show that Pumacocha $\delta^{18}O_{cal}$ reflects the average annual isotopic composition of the lake's surface waters ($\delta^{18}O_{lw}$), and that $\delta^{18}O_{lw}$ tracks the isotopic composition of precipitation ($\delta^{18}O_{precip}$), which is largely controlled by the intensity of the South American summer monsoon (SASM). Based on these relationships we use down-core $\delta^{18}O_{cal}$ measurements as a proxy for $\delta^{18}O_{precip}$ that varies with the intensity of SASM precipitation. Pumacocha $\delta^{18}O_{cal}$ increased rapidly between 11,200 and 10,300 yr B.P. from −14.5‰ to −10.5‰, reaching a maximum of −10.3‰ by 9800 yr B.P. After 9800 yr B.P., $\delta^{18}O_{cal}$ underwent a long-term decrease that tracked increasing Southern Hemisphere summer insolation, suggesting that enhanced SASM precipitation was linked to precessional forcing. Higher-frequency trends did not follow insolation and therefore represent other variability in the climate system. Millennial-scale trends from Pumacocha strongly resemble those from lower-resolution tropical Andean ice and lake core isotopic records, particularly the Huascaran ice core, and low elevation speleothems. These relationships suggest that tropical Andean isotopic records reflect variations in precipitation intensity related to precessional forcing rather than tropical temperatures. They also demonstrate a coherent pattern of SASM variability, although with differences between low elevation and Andean records during the late Glacial to Holocene transition and the late Holocene. Centennial and decadal SASM precipitation variability is also apparent. Reduced SASM rainfall occurred from 10,000–9200, 7000–5000, 1500–900 yr B.P. and during the last 100 years. Intensifications of the SASM occurred at 5000, 2200–1500, and 550–130 yr B.P. with the amplitude of variability increasing after 2200 yr B.P. These periods may represent SASM responses to ocean–atmosphere variability related to orbital and radiative forcing (e.g., El Niño-Southern Oscillation and the Intertropical Convergence Zone).

1. Introduction

Holocene South American summer monsoon (SASM) variability has been the focus of considerable research (Abbott et al., 1997a, 1997b; Abbott et al., 2003; Baker et al., 2001a; Polissar et al., 2006a; Seltzer et al., 2000; van Breukelen et al., 2008). Understanding how and why the SASM has varied through time is of interest because it is a significant source of fresh water and plays an important role in Amazonian biogeochemical cycles, including the carbon cycle (e.g., Lewis et al., 2011). The temporal resolution of past records (typically ≥100 yrs/sample), however, has limited investigations of Holocene SASM precipitation variability to orbital timescales. Furthermore, a lack of hydroclimate records from the Amazon Basin and uncertainty regarding the interpretation of Andean isotopic records with respect to temperature and precipitation has made it difficult to decipher the geographic pattern of precipitation variability over tropical South America. As a result, questions remain such as whether or not Andean oxygen isotope trends were: 1) the result of changes in rainfall over the Amazon Basin that influenced Andean isotopic records, 2) actual Andean precipitation trends, 3) changes in the integrated SASM system across both the Amazon Basin and the Andes that affected the regions equally, or 4) changes in tropical air temperatures. The first three questions stem from the fact that the isotopic composition of precipitation over tropical South America is strongly affected by the degree of rainout that occurs as moisture is transported across the Amazon Basin (Vuille and Werner, 2005). Therefore, Andean isotopic records could reflect local changes in precipitation, changes in rainfall over the Amazon Basin, or changes in rainfall over both the Andes and Amazon Basin. New low elevation speleothem records from South America have shed light on decade-scale Holocene SASM dynamics and allow for direct comparisons between low- and high-elevation isotopic records. A lack of similarly resolved records from the tropical Andes has hindered such an investigation. Discerning the relative influences of temperature

* Corresponding author.

0012-821X/$ – see front matter © 2011 Elsevier B.V. All rights reserved.
doi:10.1016/j.epsl.2011.08.040

and precipitation on Andean isotopic records has also been difficult. Previous work attributed isotopic trends in tropical Andean ice cores to variations in air temperature based in part on their similarities with Northern Hemisphere temperature records (e.g., Thompson et al., 1986). Because the direction of temperature controlled oxygen isotope fractionation in calcite is opposite to that which occurs during the formation of precipitation from water vapor, differences would be expected in the magnitude of isotopic shifts from ice core and lake calcite isotopic records of precipitation if air temperature were primarily driving the variability. At present there are no lake calcite records of the isotopic composition of precipitation from the tropical Andes, which has precluded an empirical evaluation of the relative influences of temperature and precipitation on paleoclimate timescales.

To address the above questions, we present a new decadally-resolved 11,200-year-long reconstruction of SASM rainfall based on oxygen isotope measurements of lacustrine carbonate from Laguna Pumacocha, a small lake in the central Peruvian Andes. This record provides the highest-resolution view to date of Andean hydroclimate spanning the Holocene and allows for a detailed evaluation of Holocene SASM precipitation variability, its regional expression, and the relative influence of temperature and precipitation on Andean isotopic records.

2. Study area

Pumacocha is a small alpine lake at the western edge of the Amazon Basin on the eastern flank of the Peruvian Andes at 4300 m asl (10.70° S, 76.06° W; Figs. 1 and 2a). The lake is set in a small glacial cirque with headwalls that reach a maximum elevation of 4600 m asl and a watershed area of 1.7 km^2. The catchment is currently unglaciated and there is no evidence of glaciation during the Holocene, although several large moraines that may date to the last local glacial maximum are present in the area. The lake basin is 23.5 m deep with a flat bottom and steep sides, which allows it to maintain a large volume (1.37×10^6 m^3) despite a small surface area (0.1 km^2). This morphology, together with the sheltering affect of local topography, contributes to water column stability, which is reflected by permanent stratification and anoxic conditions below ~8 m depth. Surrounding the lake is a broad marshy area between 10 and 50 m in width. This region acts as a natural sediment trap, which captures detrital carbonate that might otherwise be transported to the lake during storm events. Underlying the lake's watershed are Jurassic marine limestones of the Chambará Fm (Quispensivana, 1996). This lithology supplies significant quantities of dissolved HCO_3^- and Ca^{2+} to the lake, maintaining a surface pH of ~8, an average alkalinity of 161 mg/L HCO_3^- and saturation with respect to calcite throughout the year.

Pumacocha's climate is dominated by the SASM, with 60% of precipitation falling during the austral summer between December and March. Precipitation over the watershed averages 1000 mm yr^{-1}, which equates to 1.67×10^6 m^3 of water per year or 23% more than the lake's volume (1.36×10^6 m^3). This results in overflowing conditions throughout the year and a short residence time of a year or less.

3. Methods

3.1. Core collection

Sediment cores were retrieved from the deepest part of Pumacocha in June 2005 and August 2006 using modified piston corers (Fig. 2b). Consecutive drives were overlapped by 20.0 cm to ensure continuous recovery. Undisturbed surface sediments were captured in several freeze cores collected between August 2006 and May 2008 (Table S1). In total, 579.0 cm of sediment was retrieved. Dense glacial deposits below this depth prevented further penetration. Cores were correlated based on their physical and geochemical characteristics to form a single composite record.

3.2. Core imaging

High-resolution digital images of the sediment cores were acquired using a fixed position line-scanning digital camera with polarized full-spectrum lighting. Sediments composition was characterized by scanning electron microscopy (SEM) and X-ray diffraction (XRD).

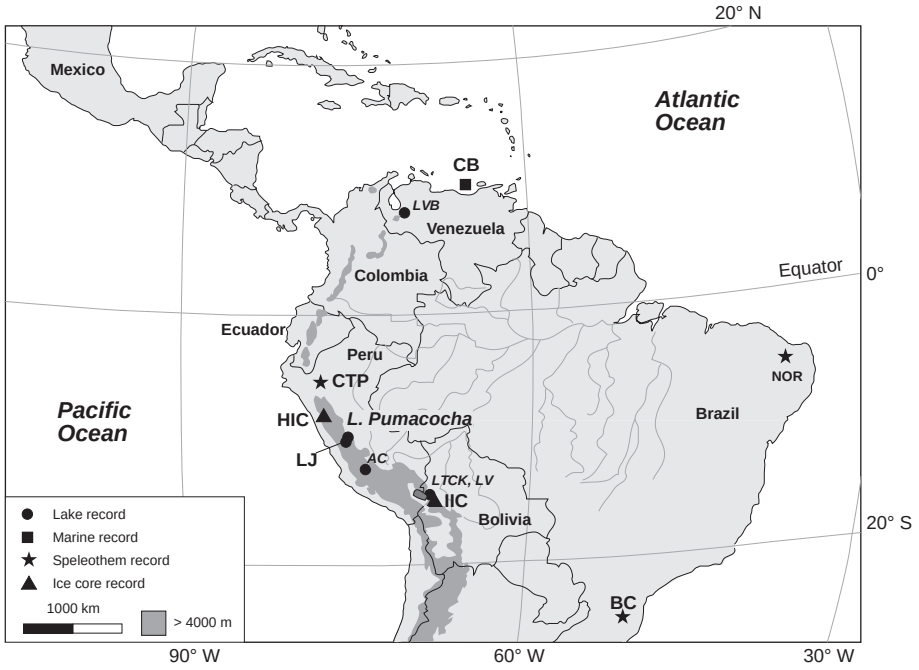

Fig. 1. Map of South American tropics with locations of sites discussed in the text. CB = Cariaco Basin, LVB = Laguna Verdes Baja, CTP = Cueva del Tigre Perdido, HIC = Huascaran ice core, LJ = Laguna Junin, AC = Laguna Azulcocha, LTCK = Laguna Taypi Chaka Kkota, LV = Laguna Viscachani, IIC = Illimani ice core, BC = Cueva Botuvera, NOR = Nordeste Region.

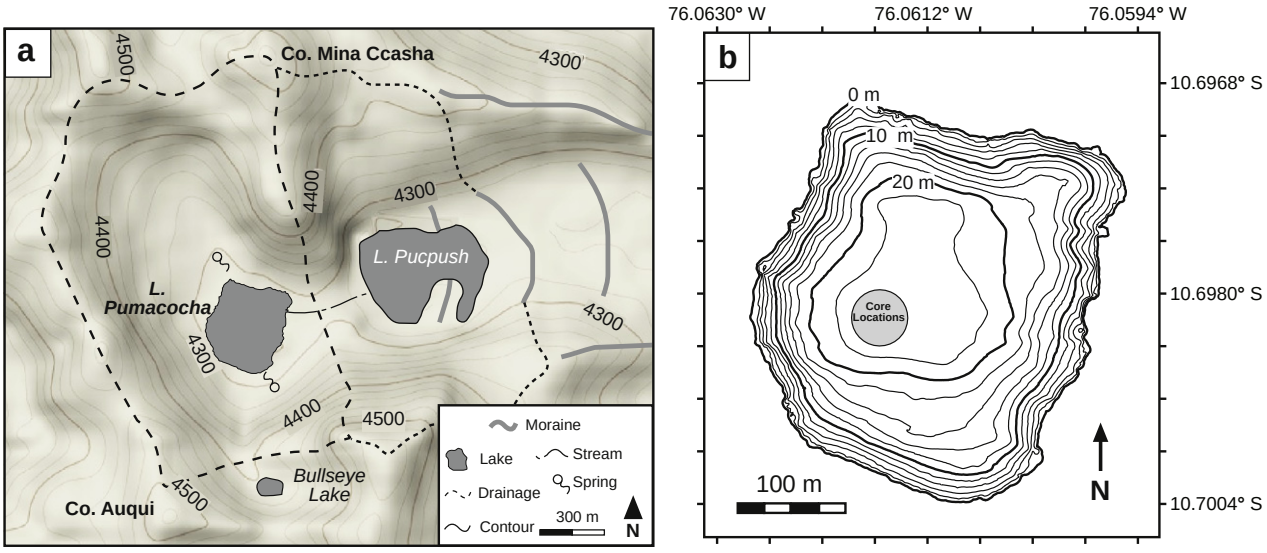

Fig. 2. Topographic map of the Pumacocha (long dash line) and Pucpush catchments (short dash line). (b) Bathymetric map of Laguna Pumacocha.

3.3. Modern sedimentation and limnology

Modern authigenic calcite was collected in sediment traps deployed in the deepest part of Pumacocha between August 2006 and May 2007 and from littoral vegetation in August 2006 and May 2008. Lake-level and surface temperatures were measured with a Solinst Levellogger deployed in a fixed position 22.25 m above the lake bottom. Air temperature and barometric pressure were measured by a land-based Solinst Barologger. All variables were measured at 4-hour intervals from May 2007 to May 2008. Temperature, pH, dissolved oxygen and specific conductivity were measured at 1 m intervals in June 2005, May 2007 and August 2008. Water samples were collected for oxygen ($\delta^{18}O_{lw}$) and hydrogen (δD_{lw}) isotope analysis between June 2005 and July 2008 with monthly sampling from August 2006 and July 2008. Samples were measured at the University of Arizona Environmental Isotope Laboratory. Reported precision is 0.1‰ for $\delta^{18}O$ and δD with values given in standard delta notation as the per mil (‰) deviation from Vienna standard mean ocean water (VSMOW). Water column alkalinity was measured in May of 2007 and 2008 using a Hach digital titrator and 1.6 N H_2SO_4.

3.4. Age control

Lead-210, ^{226}Ra and ^{137}Cs were measured at 1 cm intervals between 0.0 and 30.0 cm from freeze core D-08 by direct gamma counting (Appleby et al., 1986; Schelske et al., 1994). Eighteen radiocarbon (^{14}C) ages from Pumacocha and three ^{14}C ages from Laguna Azulcocha were determined by accelerator mass spectrometry (AMS) on selected charcoal fragments that were prepared according to standard protocols (Abbott and Stafford, 1996). AMS ^{14}C ages were calibrated to years before present (yr B.P.; present = AD 1950) with the online program CALIB 5.0 (Stuiver and Reimer, 1993). Reported ages are the 2σ median probability age with errors of the 2σ age range. The varve chronology is based on couplets counts from high-resolution digital images of freeze core B-08 and piston core C-06 to a depth of 103.5 cm following the methods of Francus et al. (2002). Four counts were completed on each core to ensure data quality and derive error estimates (1%). Varve ages are referred to in yr B.P.

3.5. Carbonate sampling and measurement

The uppermost 210 individual carbonate laminae from freeze cores B-08, B-07 and D-07 were sampled for carbonate isotope analysis ($\delta^{18}O_{cal}$ and $\delta^{13}C_{cal}$). Additional samples were collected from Livingstone cores A-05, C06, and E-06 at 1 mm intervals. Banded sections below 176.2 cm were sampled at 2.5 mm intervals.

Samples of the <63 μm sediment fraction were measured at the University of Arizona and the University of Pittsburgh. Measurements were calibrated to the NBS-19 and NBS-18 standards and are reported in standard delta notation as the per mil (‰) deviation from Vienna Pee Dee Belemnite (VPDB). Precision is ±0.1 for $\delta^{18}O$ and $\delta^{13}C$ (1σ). Replicate sample measurements yielded an internal sample reproducibility of ±0.02‰ for $\delta^{18}O_{cal}$ and ±0.03‰ for $\delta^{13}C_{cal}$.

3.5.1. Conversion of $\delta^{18}O_{cal}$ (VPDB) to $\delta^{18}O_{lw}$ (VSMOW)

Conversion of $\delta^{18}O_{cal}$ from the VPDB to the VSMOW scale was performed using the standard equation:

$$\delta^{18}O_{(VSMOW)} = 1.03091 \times \delta^{18}O_{(VPDB)} + 30.91.$$

Lake water $\delta^{18}O$ values were calculated for individual years during which the calcite samples were collected using the converted $\delta^{18}O_{cal}$ values and the equation:

$$\delta^{18}O_{H_2O_{(VSMOW)}} = \frac{\delta^{18}O_{cal(VSMOW)} + 10^3}{\alpha_{cal-H_2O}} - 10^3$$

where $\alpha_{cal\text{-}H2O}$ is the temperature dependent fractionation factor described by Kim and O'Neil (1997):

$$10^3 \ln \alpha_{cal-H_2O} = \frac{18.03 \times 10^3}{T_K} - 32.42.$$

Solinist and Hydrolab surface temperature data rounded to the nearest 0.5 °C were used to estimate the temperature of calcite formation for littoral and sediment trap calcite.

4. Results

4.1. General sedimentology

The original data presented here are archived online at the NOAA Paleoclimate Database: ftp://ftp.ncdc.noaa.gov/pub/data/paleo/paleolimnology/southamerica/peru/pumacocha2012.txt.

Light gray to tan laminated sediments composed of glacially derived detrital carbonate are present from 579.0 cm to 565.2 cm (Fig. 3; Table S2). Above 565.2 cm, there is an abrupt transition to massive black organic-rich sediments that grade into dark green to black organic-rich banded sediments by 550.0 cm depth. Above 460.0 cm, the sediments become a light tan color. Between 550.0 and 176.2 cm depth, there are three sections with laminated sediments from 550.0 to 440.0 cm, 365.0 to 361.7 cm and 211.5 to 210.0 cm. At 176.2 cm, the sediments become finely laminated with the exception of four discrete banded intervals that are dark green in color.

4.2. Couplet sedimentology

High-resolution digital imagery, SEM, and XRD indicate that the couplets between 176.2 and 0.0 cm consist of discrete dark green organic-rich layers overlain by tan to white layers of euhedral calcite crystals (Fig. 3c and d). Couplet structure and compositional regularity suggest seasonally rhythmic deposition in the uppermost portion of the Pumacocha record. Distinct couplet sequences are easily correlated among the network of cores from Pumacocha, demonstrating that sedimentation is consistent across the lake bottom.

4.3. Age control

The AD 1963 ^{137}Cs maximum occurs between 8.7 and 10.5 cm in freeze core D-08 (Fig. 4; Table S3). Based on the mean depth of this radiometric marker, we estimate a sedimentation rate of 0.21 cm yr^{-1}. The depth interval containing the AD 1963 ^{137}Cs peak also contains the AD 1963 couplet determined by couplet counting. The sedimentation rate based on the mean depth of the AD 1963 couplet (0.20 cm yr^{-1}) agrees with the ^{137}Cs-determined sedimentation rate.

Six AMS ^{14}C ages were measured on charcoal fragments from the upper 104.5 cm of the Pumacocha record (Fig. 5; Table S4). The four lower ages, despite one being reversed, are in good agreement with the couplet-count-based ages (Fig. 5). Age reversals within the core may be the result of sample contamination by aquatic or littoral vegetation and/or the presence of 'old carbon' washed into the lake from the watershed.

Excess ^{210}Pb activities vary about a mean between 0.0 and 8.7 cm and then decrease exponentially (Fig. 4). Application of a linear accumulation model below the plateau region yields an accumulation rate

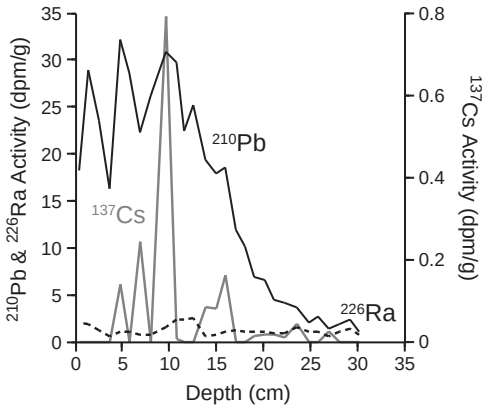

Fig. 4. Plot of activities for excess ^{210}Pb (solid black solid), ^{226}Ra (dashed black line; i.e., supported ^{210}Pb), and ^{137}Cs (solid gray line).

of 0.35 cm yr^{-1} (Appleby and Oldfield, 1983), which is higher than the accumulation rates estimated from ^{137}Cs and couplet counts and underestimates the age of the ^{137}Cs peak. Non-decreasing excess ^{210}Pb activities in surface sediments are usually attributed to sediment mixing, either from bioturbation or coring disturbances (Appleby and Oldfield, 1983). However, the Pumacocha sediments are finely laminated to the sediment–water interface, precluding such influences. Constant ^{210}Pb activities in surface sediments, despite no physical mixing, have been observed in other varved lakes (e.g., Erten et al., 1985) and attributed to a mobile ^{210}Pb fraction at the dissolved and/or colloid level that moves quickly through surface pore waters until compaction precludes interstitial pore fluid movement (Abril, 2003). This process may affect ^{210}Pb while not altering the ^{137}Cs profile (Abril, 2003). Because the ^{210}Pb profile appears to be compromised by the processes described above, it was not utilized for age control.

The agreement between the ^{137}Cs, AMS ^{14}C and couplet counts supports the idea that the couplets preserved in the Pumacocha sediment core are varves. We therefore rely on varve ages in the upper 103.5 cm of the Pumacocha sediment record. Below 103.5 cm, we fit a 4th order polynomial to the remaining 12 AMS ^{14}C ages (Fig. 5).

4.4. Modern $\delta^{18}O_{lw}$

The 27 monthly surface water samples from Pumacocha plot along a Local Meteoric Water Line (LMWL) that parallels, but is offset from,

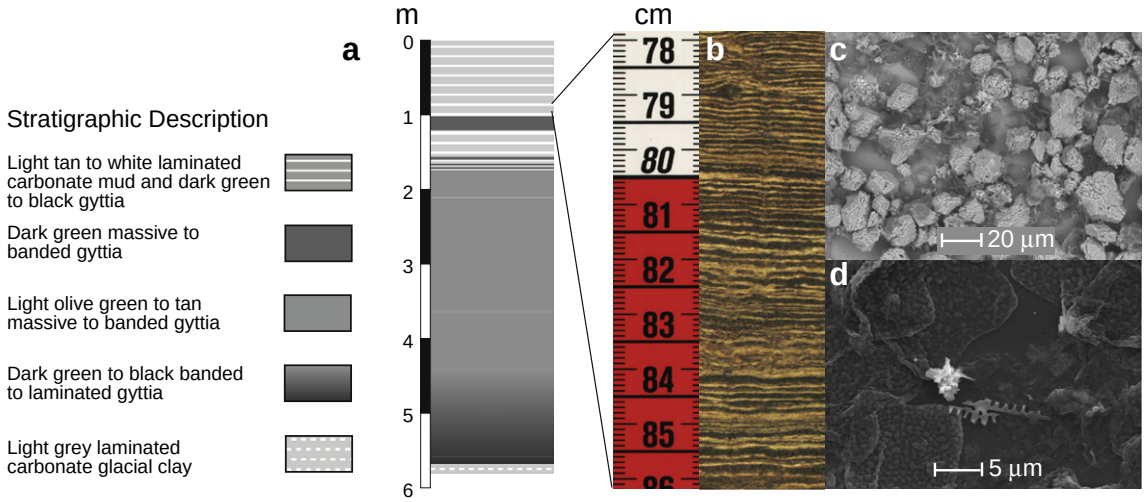

Fig. 3. (a) Stratigraphic column of the Pumacocha sediment record. (b) A high-resolution digital image from the upper portion of the Pumacocha sediment record showing a typical section of finely laminated millimeters scale varves. Representative SEM images showing the (c) euhedral calcite crystals that comprise the sediments in the light lamina and the (d) organic matter that comprises the dark lamina from the varved portion of the Pumacocha record.

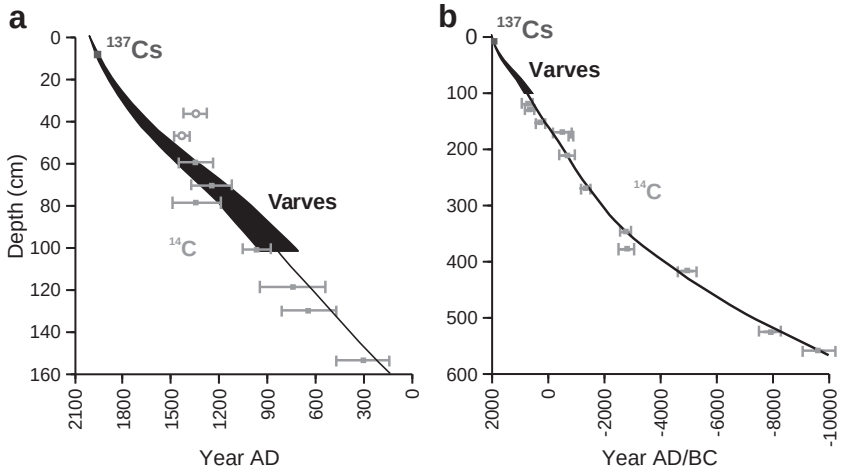

Fig. 5. The left graph shows the varve-^{137}Cs-^{14}C age model for the upper 160 cm. Ages based on couplet counts have an estimated error of +/− 1% (shown with the increasing error range in black). Error ranges for ^{14}C are shown with horizontal bars for ages, and vertical bars for depth. The right graph shows the entire age model for the last 11,500 years. A 6th order polynomial was fit to these data to derive the final age depth model.

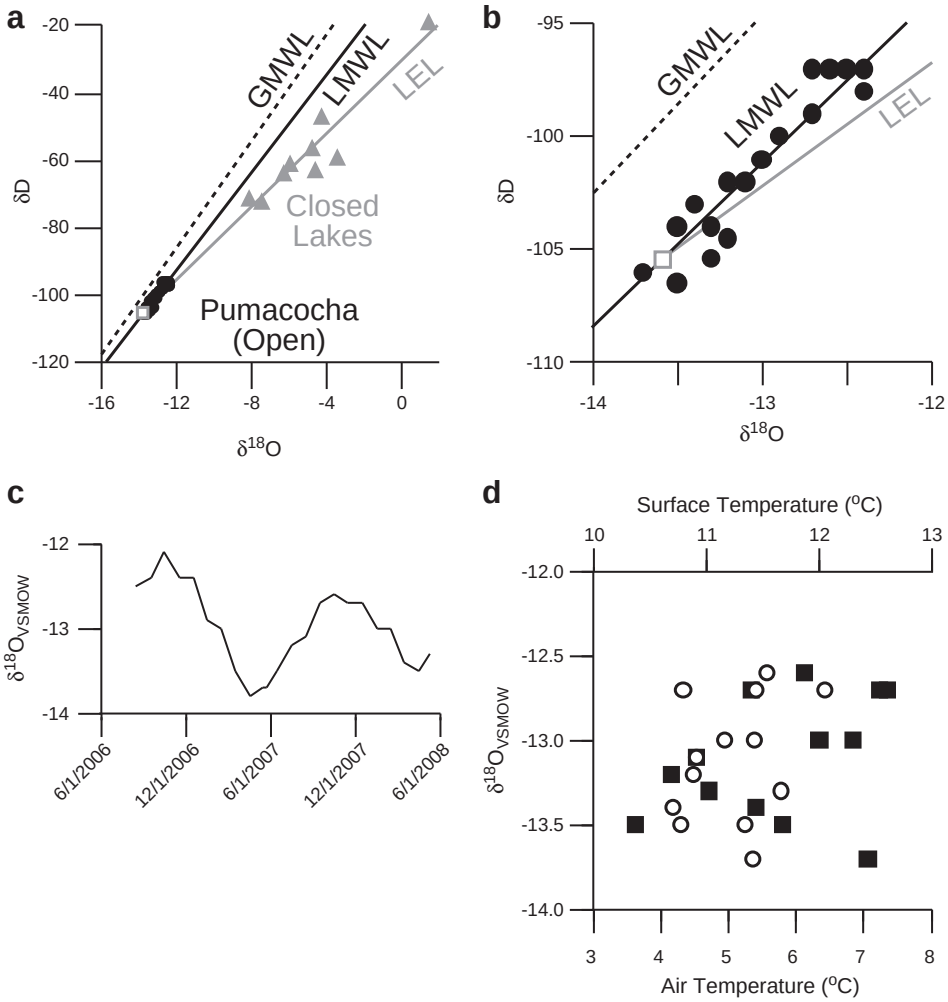

Fig. 6. (a) Surface water samples from Pumacocha (black circles) plotted with surface water samples from regional hydrologically closed basin lakes (gray triangles) in $\delta^{18}O$–δD (VSMOW) space. The Pumacocha surface water samples plot along a Local Meteoric Water Line (LMWL; black line) that parallels the Global Meteoric Water Line (GMWL; dashed line). Regional lakes with closed basin hydrologies plot along a Local Evaporation Line (LEL; gray line), which is oblique to both the LMWL and the GMWL and intersects the LMWL at − 13.6‰ (gray square). (b) Same as in (a) but expanded to show that isotopic variability in the Pumacocha surface water samples tracks a LMWL that is parallel to the GMWL and oblique to the LEL. (c) Monthly $\delta^{18}O_{lw}$ (VSMOW) measurements of Pumacocha surface waters plotted versus time. (d) $\delta^{18}O_{lw}$ (VSMOW) of monthly surface water samples from Pumacocha versus surface air temperatures (circles) and lake surface temperatures (squares).

Table 1
Equations for the Global Meteoric Water Line (GMWL), the Local Meteoric Water Line (LMWL) Local Evaporation Line (LEL). Also shown is the $\delta^{18}O$ value where the LEL intersects the LMWL (LMWL = LEL). All r^2 are significant above the 95% confidence interval.

Line	Equation	r^2
GMWL	$\delta D = 7.96\ (\delta^{18}O) + 8.86$*	
LMWL	$\delta D = 7.24\ (\delta^{18}O) - 7.07$	0.90
LEL	$\delta D = 5.43\ (\delta^{18}O) - 31.72$	0.89
LMWL = LEL	−13.6‰ $\delta^{18}O$	

* Rozanski et al. (1993).

the Global Meteoric Water Line (GMWL; Fig. 6; Table 1; Rozanski et al., 1993). These samples also show a strong seasonal oscillation where $\delta^{18}O_{lw}$ varied the most between 2006/2007 (1.7‰); $\delta^{18}O_{lw}$ was −12.1‰ during October 2006 and −13.8‰ in April 2007. Less $\delta^{18}O_{lw}$ variability (0.9‰) occurred in 2007/2008; $\delta^{18}O_{lw}$ was −12.6‰ in October 2007 and −13.5‰ in April 2008.

4.5. Modern carbonate

Authigenic calcite collected from Pumacocha's littoral zone in August 2006 and May 2008 exhibited $\delta^{18}O_{cal}$ values of −12.2‰ and −12.4‰, respectively. Sediment trap $\delta^{18}O_{cal}$ averaged −12.8‰ between August 2006 and May 2007 with a maximum of −12.4‰ and a minimum of −13.2‰. Converted from VPDB to VSMOW (−13.0‰), modern $\delta^{18}O_{cal}$ is identical with annual average $\delta^{18}O_{lw}$ for the respective time periods when the calcite was recovered (−13.0‰ VSMOW).

4.6. Holocene $\delta^{18}O_{cal}$

Pumacocha $\delta^{18}O_{cal}$ increased rapidly between 11,200 and 10,300 from −14.5‰ to −10.5‰ (Fig. 7). After 10,300 yr B.P., $\delta^{18}O_{cal}$ remained high with peak values of −10.3‰ at 9800 yr B.P. Subsequently, $\delta^{18}O_{cal}$ decreased gradually, reaching a minimum of −15.8‰ by 370 yr B.P. After 370 yr B.P. $\delta^{18}O_{cal}$ generally increased to the present, particularly during the last 100 years. Notably, $\delta^{18}O_{cal}$ variability increased greatly after ~2200 yr B.P., which coincides with the transition from banded to finely laminated sediments (Fig. 7). Decadal to centennial scale variability is also apparent in the Holocene Pumacocha $\delta^{18}O_{cal}$ record. Increased $\delta^{18}O_{cal}$ occurred from 10,000–9200, 7000–5000, and 1500–900 yr B.P. Decreased $\delta^{18}O_{cal}$ occurred at 5000, 2200–1500, and 550–130 yr B.P.

5. Discussion

5.1. Interpretation of the Pumacocha $\delta^{18}O_{cal}$ record

Oxygen isotope ratios of authigenic lacustrine calcite are a function of the initial $\delta^{18}O_{lw}$ and the temperature at which the calcite is precipitated (Kim and O'Neil, 1997; O'Neil et al., 1969). Lake surface temperatures at Pumacocha varied by 1.2 °C between June 2007 and May 2008, which would shift $\delta^{18}O_{cal}$ by ~0.3‰ (Kim and O'Neil, 1997). Sediment trap $\delta^{18}O_{cal}$ varied by 0.8‰ during this same interval, which is nearly twice that explainable by temperature-controlled fractionation alone, suggesting that temperature is not the dominant driver of modern $\delta^{18}O_{cal}$ variability. Temperature also appears to play a negligible role in $\delta^{18}O_{cal}$ variability during the past. Although estimating temperature changes during the Holocene is difficult, the Little Ice Age (LIA) from ~650 to 130 yr B.P. appears to have been one of the coolest periods in the last 10,000 years with the largest ice advance since the late Glacial (Rabatel et al., 2005; Rabatel et al., 2008; Solomina et al., 2007). Importantly, the Pumacocha watershed and sediment record show no evidence for Holocene glaciation, which could compromise the $\delta^{18}O_{cal}$ record by introducing detrital carbonate. This is consistent with work that suggests headwalls below 5000 m asl were not glaciated during the LIA (Rodbell et al., 2008). South American temperatures during the LIA have been estimated from changes in lake productivity in central Chile (0.7 to 0.9 °C; von Gunten et al., 2009) and reductions in glacier equilibrium line altitudes in the Cordillera Real, northern Bolivia (1.1 to 1.2 °C; Rabatel et al., 2008). Accounting for temperature controlled $\delta^{18}O$ fractionation during the formation of precipitation from water vapor (~+0.6‰ per °C; ref. Rozanski et al., 1992) and calcite from lake water (−0.24‰ per °C; Kim and O'Neil, 1997), cooling of between 0.7 and 1.2 °C would lower $\delta^{18}O_{cal}$ at Pumacocha by 0.25 to 0.43‰. This is considerably smaller than the observed 2‰ lowering relative to the present, which would require nearly a 6 °C drop in temperature. Additionally, the 5.6‰ difference in Pumacocha $\delta^{18}O_{cal}$ between the early Holocene maximum and LIA minimum would require an almost 16 °C temperature decrease during the Holocene. These temperature variations are far too large to be realistic, particularly in light of recent work suggesting that Amazonian temperature anomalies have not exceeded ±2 °C during the Holocene (van Breukelen et al., 2008). Factors other than temperature must therefore be invoked to account for the trends and degree of isotopic variability in the Pumacocha $\delta^{18}O$ record.

Additional influences on a lake's isotopic mass balance include the isotopic composition of its inflows (i.e., groundwater, precipitation and surface water) and outflows (i.e., groundwater seepage, evaporation and surface outflow). As a cirque lake in a perched catchment that is topographically isolated from nearby watersheds, local and regional groundwater may be excluded as influences on Pumacocha's isotopic mass balance. Surface water isotopic variability can also be excluded because Pumacocha is a headwater lake with no fluvial inputs whose hydrologic mass balance is dominated by precipitation during the monsoon season from December through March. Evaporative modification of Pumacocha's surface waters also appears to play a minimal role in the lake's hydrologic and isotopic mass balances. Fig. 6 shows that Pumacocha's surface waters plot on a Local Meteoric Water Line (LMWL) that is offset from, but parallel to the Global Meteoric Water Line (GMWL), indicating minimal evaporative modification of the lake's isotopic mass balance. If Pumacocha's surface waters were influenced by evaporation, they would plot along the Local Evaporation Line (LEL), which is constrained by surface water samples from regional closed basin lakes (Fig. 6). The limited influence of evaporation on $\delta^{18}O_{lw}$ is further supported by the close agreement between predicted mean $^{18}O_{precip}$ based on interpolated IAEA-GNIP data (−12.9 ± 1.5‰; Bowen and Wilkinson, 2002; Bowen et al., 2005) and average $\delta^{18}O_{lw}$ at Pumacocha from June 2005 to July 2008 (−13.0‰). Together, these results strongly suggest that Pumacocha's isotopic mass balance is dominated by variations in the isotopic composition of precipitation falling at the lake site.

Oxygen isotope measurements of modern Pumacocha calcite demonstrate a clear relationship between $\delta^{18}O_{cal}$ and $\delta^{18}O_{lw}$. For comparison with $\delta^{18}O_{lw}$, modern $\delta^{18}O_{cal}$ values were converted to

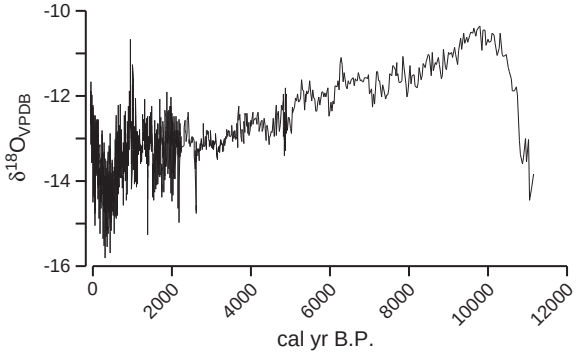

Fig. 7. Plot of $\delta^{18}O_{cal}$ from Pumacocha between 11,200 and −57 yr.

the VSMOW scale. Both the annual- and three-year-averages of these converted $\delta^{18}O_{cal}$ values are identical within error to the $\delta^{18}O_{lw}$ corresponding to the time of calcite formation (Bird et al., 2011). These results indicate that calcite precipitated at Pumacocha is in isotopic equilibrium with lake water and that it faithfully captures variations in $\delta^{18}O_{lw}$ through time. This relationship appears to have been consistent throughout the Holocene based in part on the lack of covariance between $\delta^{18}O_{cal}$ and $\delta^{13}C_{cal}$ during the entire 11,200-year-long record (Li and Ku, 1997). Even during periods of enhanced aridity in the tropical Andes, such as the early Holocene (10,700–8300 yr B.P.), the $\delta^{18}O$–$\delta^{13}C$ relationship remained poor. This evidence indicates that Pumacocha $\delta^{18}O_{lw}$ is linked to changes in $\delta^{18}O_{precip}$ and that the Pumacocha $\delta^{18}O_{cal}$ record may be used to infer variations in $\delta^{18}O_{precip}$ through the Holocene.

The isotopic composition of precipitation over tropical South America is primarily controlled by Raleigh-type fractionation during rainout (Vuille and Werner, 2005). Observations show that $\delta^{18}O_{precip}$ is lower during the austral summer wet season, despite warmer temperatures, and higher during the dry austral winter, when temperatures are generally cooler (Vuille et al., 2003a). Year-to-year $\delta^{18}O_{precip}$ variability investigated with observational and proxy data and stable isotope-enabled global climate models shows that $\delta^{18}O_{precip}$ is directly related to the intensity of the SASM with lower values occurring during intense monsoon seasons, and vice versa (Vuille and Werner, 2005). This isotopic response to precipitation intensity is preserved and enhanced along the trajectory of an air mass. Therefore, an isotopic record of precipitation (i.e., Pumacocha) that is located downstream from the core precipitation region is significantly correlated with the cumulative intensity of precipitation along the trajectory of that air mass. This is true regardless of whether or not the timing and amount of precipitation at the site differs slightly from that which characterizes the core region of convective activity, in this case the Amazon Basin (Vuille and Werner, 2005). This results in $\delta^{18}O_{precip}$ being more spatially coherent and reflective of the overall intensity of precipitation than the amount of local precipitation itself, which is strongly affected by microclimatic effects (Schmidt et al., 2007). This "isotopic memory" of an air mass and its influence on downstream $\delta^{18}O$ records, such as Pumacocha, means that local isotopic records of precipitation can be used to infer large-scale changes in the intensity of precipitation over tropical South America (Vuille and Werner, 2005). Accordingly, we interpret $\delta^{18}O_{cal}$ from Pumacocha as a proxy for the intensity of precipitation over Andean tropical South America.

Our interpretation of the Pumacocha $\delta^{18}O_{cal}$ record is supported by statistically significant relationships with records of the isotopic composition of precipitation from tropical Andean ice cores. The Pumacocha $\delta^{18}O_{cal}$ trends are strikingly similar in direction and magnitude to the independently dated Huascaran and Illimani ice cores (Fig. 7; Table 2). While it could be argued that early Holocene aridity influenced these records via sublimation/evaporation, it has been shown that ice core records are not significantly affected by isotopic enrichment through sublimation (Hardy et al., 1998). At Pumacocha, the evidence suggests that the lake has been hydrologically open throughout the period represented by the $\delta^{18}O_{cal}$ record, including the early Holocene. Given evidence that temperature does not contribute greatly to $\delta^{18}O_{cal}$ variability at Pumacocha, the strong and significant correlations with South American ice cores during the Holocene strongly suggests that these records are all recording changes in the isotopic composition of precipitation driven by changes in the intensity SASM precipitation through Raleigh-type fractionation, not temperature. Although in contrast to previous studies that attributed isotopic variability in tropical ice cores to temperature (Thompson et al., 2000), this conclusion is consistent with multiple lines of evidence that indicate precipitation intensity is the primary control on isotopic records of precipitation from the tropical Andes (Hastenrath et al., 2004; Hoffmann et al., 2003; Vuille et al., 2003b). While the Holocene scale $\delta^{18}O$ trends documented here cannot be explained by local temperature changes, global and hemispheric temperatures likely play an important role in driving SASM variability. This idea is supported in part by the close relationship between Pumacocha $\delta^{18}O_{cal}$ and reconstructed Northern Hemisphere temperatures during the last 2000 years (Bird et al., 2011; Moberg et al., 2005) and is consistent with global climate model simulations that show monsoon intensities are affected by interhemispheric temperature gradients (Liu et al., 2003).

Table 2
Correlation coefficients of comparisons between Andean paleoclimate archives. All r^2 are significant above the 95% confidence interval.

	10,000 yr B.P. to present	11,200 yr B.P. to present
Pumacocha vs. Huascaran	0.77	0.79
Pumacocha vs. Illimani	0.73	
Pumacocha vs. L. Verdes Baja	0.64	
Huascaran vs. Illimani	0.69	

5.2. Holocene Andean $\delta^{18}O_{precip}$ trends

Pumacocha $\delta^{18}O_{cal}$ increased rapidly during the early Holocene between 11,200 and 10,300 yr B.P., reaching a maximum of −10.3‰ by 9800 yr B.P. This trend is also apparent in the independently dated Huascaran and Illimani ice core records, which indicates that an abrupt climate event during the late Glacial to Holocene transition, not clearly linked to precessional insolation forcing, affected the southern and central tropical Andes. This event may be driven in part by high-latitude influences related to ice-sheet and ocean–atmosphere dynamics. The transition from low to high $\delta^{18}O$ and δD in these records during the late Glacial to Holocene transition may suggest that the SASM was strong over the central and southern tropical Andes during this time and abruptly decreased in strength, with minimum precipitation by 9800 yr B.P. Isotopic evidence from Lake Junin, an evaporatively influenced lake in the central Peruvian Andes, however, suggests that evaporation was high in the tropical Andes during the late Glacial to early Holocene transition when $\delta^{18}O$ and δD were low in the Pumacocha and ice core records (Seltzer et al., 2000). This may indicate reduced effective moisture in the tropical Andes during this time.

After 9800 yr B.P., $\delta^{18}O_{cal}$ underwent a long-term decrease (−0.31‰ per millennium), suggesting that SASM precipitation steadily strengthened throughout Holocene (Fig. 8d). As noted previously, these Holocene-scale trends are statistically similar to those observed in the Huascaran and Illimani ice core records. This indicates that Pumacocha $\delta^{18}O_{cal}$ is representative of the isotopic composition of precipitation across the central and southern tropical Andes, and that long-term reductions in evaporation during the Holocene in response to strengthening of the SASM (Seltzer et al., 2000) did not strongly influence the Pumacocha $\delta^{18}O_{cal}$ signal (Fig. 8d and e).

The Pumacocha record also exhibits strong and significant correlations with a diatom opal $\delta^{18}O$ record from Laguna Verdes Baja (LVB; 8.86° N, 70.87° W; 4170 m asl), a small alpine lake in the Northern Hemisphere Venezuelan Andes (Fig. 8a and d; Table 2; Polissar et al., 2006a). The correlation with LVB is particularly remarkably because it suggests that Holocene SASM variability similarly affected the greater tropical Andes, regardless of hemispheric differences in the seasonal distribution of insolation on precessional timescales (Fig. 8a and d; Table 2). This points to a mechanism that is capable of affecting the large-scale strength of the SASM in both hemispheres.

Multi-decadal and centennial $\delta^{18}O_{cal}$ variability is also apparent in the Pumacocha record. Notable periods of high $\delta^{18}O_{cal}$ suggesting weak SASM precipitation characterize the Pumacocha record from

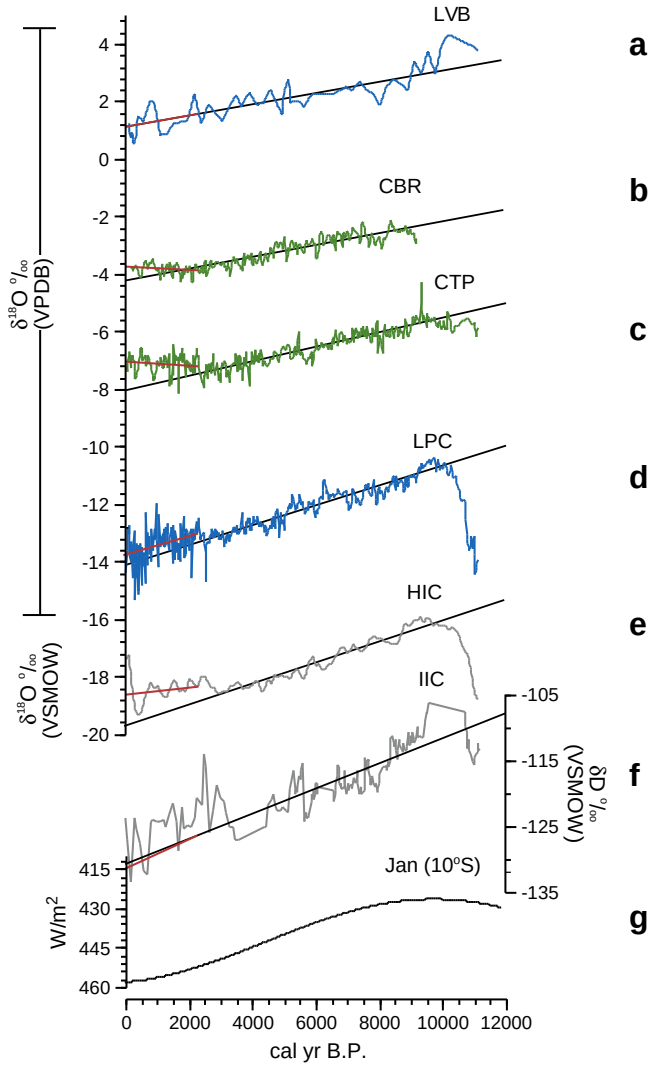

Fig. 8. Comparison of tropical South American isotopic records from (a) Laguna Verdes Baja, VE, (b) Caverna Botuvera, PE (CBR), (c) Cueva del Tigre Perdido, PE (CTP), (d) Laguna Pumacocha, PE (LPC), (e) Huascaran ice core, PE (HIC), and (f) Illimani ice core, BO (IIC). The black line in each profile is the calculated slope from 10,000 to 2200 cal yr B.P. and the red line is the slope calculated from 2200 cal yr B.P. to the present. (g) January insolation at 10° S during the last 12,000 years with the y-axis *reversed* so that increasing insolation plots toward the bottom. Records from lakes are shown in blue, speleothems in green, and ice cores in gray. (For interpretation of the references to color in this figure legend, the reader is referred to the web version of this article.)

10,000–9200, 7000–5000, 1500–900 yr B.P. and during the last 100 years. The period of high $\delta^{18}O_{cal}$ between 7000 and 5000 yr B.P. is particularly significant because it corresponds to a low stand at Lake Titicaca from 7500 to 5000 inferred from seismic profiling and sediment $\delta^{13}C$ (Row et al., 2003; Seltzer et al., 1998). This may indicate that drier conditions affected the tropical Andes during the middle Holocene. However, additional records sensitive to evaporation are needed to test this idea. Periods of low $\delta^{18}O_{cal}$ in the Pumacocha record suggest that enhanced SASM precipitation occurred primarily during the middle and late Holocene after 5000 yr B.P., particularly between 2200–1500, and 550–130 yr B.P. The transition to wetter conditions at 5000 yr B.P. following drier middle Holocene conditions is significant because several records from the tropical Andes show a pronounced climate change at this time. In particular, there is evidence that the ice cap at Quelccaya was reestablished at this time and that water levels at Lake Titicaca increased (Baker et al., 2001b; Thompson et al., 2006). A previously unpublished lake sediment core from Laguna Azulcocha (12.07° S, 75.67° W; 4450 m asl; 160 km south of Pumacocha) provides further evidence that precipitation increased at 5000 yr B.P. Currently an 11 m deep headwater lake with a small watershed (<1 km^2), Azulcocha was dry prior to 5400 yr B.P., supporting drier regional conditions middle Holocene (Fig. S1; Table S5). Between 5400 and 5000 yr B.P. there was an abrupt onset of lacustrine sedimentation, and by 4400 yr B.P. the sediments were finely laminated, suggesting deep-water conditions. The decrease in Pumacocha $\delta^{18}O_{cal}$ at 2200 yr B.P. is also recognized in other Andean records, including further increases in lake levels at Titicaca, as well as lake level increases and the onset or neoglaciation at Lago Taypi Chaka Kkota and Laguna Viscachani in the Cordillera Real of Bolivia (Abbott et al., 1997a; Abbott et al., 1997b). The return to drier conditions in the Andes between 1500 and 900 yr B.P. with peak aridity between 1100 and 900 yr B.P. is less well documented in Andean records because very few records with sufficient temporal resolution cover this period. Bird et al. (2011), however, described this event in detail and linked it with the Northern Hemisphere Medieval Climate Anomaly and a northward position of the Atlantic Intertropical Convergence Zone (ITCZ). The pronounced decrease in Pumacocha $\delta^{18}O_{cal}$ between 550 and 130 yr B.P. occurred during the LIA, a prominent climate anomaly in many Andean records from both hemispheres. This event was associated with glacial advances, cooler temperatures and significantly increased precipitation, which was likely in response to a southward displacement of the Atlantic ITCZ (Polissar et al., 2006b; Bird et al., 2011). Following the LIA pluvial phase, Pumacocha $\delta^{18}O_{cal}$ showed a strong upward trend that is also captured in the Huascaran and Quelccaya ice cores, suggesting a return to drier conditions.

The robust relationships between ice core and lacustrine isotopic profiles demonstrate that these geological archives reflect broadly uniform changes in the isotopic composition of precipitation across the tropical Andes during the Holocene (Fig. 8a–f). Given the superior resolution of the Pumacocha record (~20 yrs/sample from 2200 to 11,200 yr B.P. and 1.25 yrs/sample from −57 yr B.P. to 2200 yr B.P.), we use this record to examine isotopic shifts in South American precipitation during the last 11,200 years by comparing it with low elevation speleothem $\delta^{18}O_{cal}$ records.

5.3. Holocene $\delta^{18}O$ trends in SASM precipitation

Long-term changes in the isotopic composition of precipitation over South America are controlled by many factors including the isotopic composition of source waters (i.e., the tropical Atlantic), the degree of rainout during transport, moisture recycling across the Amazon Basin and altitude affects as moisture is uplifted to and across the Andes (Vuille and Werner, 2005; Sturm et al., 2007). Polissar et al. (2006a) examined the influence of these processes on $\delta^{18}O_{precip}$ reaching the Andes through the Holocene using a simple model calibrated to modern climatic boundary conditions. They concluded that Holocene reductions in $\delta^{18}O_{precip}$ likely resulted from less effective lowland moisture recycling, which increased runoff and reduced the fraction of moisture reaching the Andes. While insightful, this study was limited by a lack of lowland hydroclimate records, which are essential to test this hypothesis.

New speleothem records from north and southeastern Brazil (Wang et al., 2007; Cruz et al., 2009) and the western Amazon Basin (van Breukelen et al., 2008) now allow for a direct comparison of highland and lowland hydroclimate on millennial to centennial timescales (Fig. 8b and c). Speleothems from the 'Nordeste' region of northeastern Brazil (05.60° S, 37.73° W; 100 m asl) show that precipitation in this region is anti-phased with the rest of tropical South America (Cruz et al., 2009). Through the Holocene, 'Nordeste' precipitation decreased, as indicated by a long-term trend toward more positive $\delta^{18}O_{cal}$. In the western Peruvian Amazon, a speleothem $\delta^{18}O$ record from Cueva Tigre del Perdido (CTP; 5.94° S, 77.30° W; 1000 m asl) provides a record of $\delta^{18}O_{precip}$ that incorporates the

isotopic modification of precipitation by rainout and water recycling over the Amazon, but is free of other influences that affect Andean $\delta^{18}O_{precip}$ records (van Breukelen et al., 2008). The CTP record shows a long-term Holocene decrease in $\delta^{18}O_{precip}$ that is similar to Holocene $\delta^{18}O_{precip}$ trends from a speleothem record from Caverna Botuvera, southeastern Brazil (27.23° S, 49.15° W; 250 m asl), illustrating that the CTP record reflects large-scale hydrologic conditions across the Amazonian lowlands (Fig. 8b and c). For this reason, we use the CTP record for comparison with the Pumacocha $\delta^{18}O_{cal}$ record.

Both the CTP and Pumacocha $\delta^{18}O_{cal}$ records show a general trend of high $\delta^{18}O_{cal}$ during the early Holocene with a long-term decrease to minimum values during the late Holocene ($r^2 = 0.67$, $p<0.05$). Important differences occur, however, during the late Glacial to early Holocene transition and the late Holocene. From 11,200 to 10,300 yr B.P., the CTP records suggest that $\delta^{18}O_{precip}$ over the Amazon Basin remained high with no abrupt changes during this time, while the Pumacocha record shows an abrupt $\delta^{18}O_{cal}$ increase (Fig. 8). This suggests that precipitation over the Andes may have been considerably greater than that over the Amazon Basin from 11,200 to 10,300 yr B.P., despite enhanced evaporation, and that Andean precipitation weakened to a greater extent during the early Holocene. During the late Holocene, the long-term decrease in CTP $\delta^{18}O_{cal}$ reverses direction at ~2200 yr B.P., showing a slight increasing trend to the present. This is in contrast to the Pumacocha record that shows a sustained decrease in $\delta^{18}O_{cal}$ that was not reversed until 50 yr B.P. (Fig. 8d). The low elevation $\delta^{18}O_{precip}$ slope reversal suggests that precipitation may have decreased slightly over the Amazon Basin during the last 2200 years while Andean precipitation continued to increase.

On multi-decadal and centennial timescales, the Pumacocha and CTP records have similar trends, although with several differences in the timing and magnitude of isotopic shifts. These differences may be caused in part by age models and/or sampling differences. For example, the resolution of the CTP record decreases after 1300 yr B.P. and as a result the Medieval Climate Anomaly and LIA are not well resolved. Higher temporal resolution cave records, such as the near-annually resolved 1000-year-long Cascayunga Cave record, do show a clear LIA signal with isotopic shifts synchronous to those at Pumacocha, supporting the idea that this event was coherent and regionally extensive (Bird et al., 2011; Reuter et al., 2009). No doubt, knowledge of Holocene SASM variability will improve as more high-resolution isotopic records are produced. The overall visual correspondence between the Pumacocha and CTP records is quite strong, however, suggesting that multi-decadal and centennial SASM variability may be largely coherent over the Amazon Basin and Andes and subject to similar forcing mechanisms.

The strong regional similarities of hydrologic transitions across the Andes and Amazon Basin suggest a common forcing mechanism. Although it has been assumed that orbital forcing cannot account for the coherent trends in South American precipitation because opposite responses would be expected for the different hemispheres (Polissar et al., 2006a), the consistent isotopic response of Andean records from both hemispheres on precessional timescales supports a leading role for orbital forcing in driving the transition to progressively wetter conditions through the Holocene. This idea is in accord with model simulations that show monsoons are strongest in the hemisphere with maximum summer insolation (Liu et al., 2003) and with results from an isotope enabled atmospheric climate model that show that orbital changes in insolation affect the strength of convergence and precipitation equally over the northern and southern tropical Andes (Cruz et al., 2009). That the Cariaco Basin %Ti record is anthiphased with the Andean isotope records and model simulations suggests that it may not reflect precipitation over the northern South American Andes, but instead captures precipitation variability along the coast of northern tropical South America.

The mechanisms behind decadal to multi-centennial Holocene SASM variability are more complex and less clear than those that appear to act on millennial timescales. This higher-frequency variability may reflect the combined influence of various forcing mechanisms, including the extent and distribution of sea ice (Hodell et al., 2001), variations in the latitude of the ITZC (Liu et al., 2003; Bird et al., 2011), changes in Earth's radiative budget from variations in solar irradiance and volcanism (Jones and Mann, 2004) and ocean–atmosphere responses (e.g., El Niño-Southern Oscillation; ENSO) to orbital-scale changes in the distribution of insolation (Clement et al., 2000; Emile-Geay et al., 2007). Because of the complex nature of high-frequency Holocene SASM variability, global climate model simulations that integrate ocean–atmosphere–cryosphere responses to multiple forcings that act on a range of time scales are required to better understand the potentially unique nature of these abrupt climate events.

6. Summary and conclusions

The work presented here focuses on a new decadally resolved reconstruction of SASM precipitation based on $\delta^{18}O_{cal}$ measurements of authigenic calcite from a small alkaline lake in the central Peruvian Andes that spans the last 11,200 years. The results show a complex, but consistent, history of SASM precipitation variability that is characterized by both abrupt and long-term changes in the strength of the SASM. During the late Glacial to Holocene transition, Pumacocha $\delta^{18}O_{cal}$ increased abruptly, a trend captured by independently dated Andean ice core records from Nevados Huascaran and Illimani. Maximum $\delta^{18}O_{precip}$ during the early Holocene indicates that SASM precipitation was considerably reduced during this time. Following early Holocene aridity, precipitation gradually increased throughout the Holocene. The long-term trends in the Pumacocha record are statistically similar to trends in the Huascaran and Illimani ice core records, tropical Andean lake records from both hemispheres, and low elevation speleothem records from the Amazon Basin. The strong relationships between these independent isotopic records, particularly Pumacocha and Huascaran, indicate that isotopic records from tropical South America reflect changes in precipitation intensity, not tropical temperatures, and that SASM precipitation trends of the same sign were essentially synchronous across the continent. The complex, yet consistent shape of each of these records further indicates that common forcing mechanisms acting on a range of timescales drove the observed isotopic variability. The coherent millennial-scale SASM precipitation trends in these records are likely a response to increasing Southern Hemisphere summer insolation, which enhanced convection over the central and western Amazon Basin while increasing subsidence to the east. Low elevation speleothems from the eastern Peru and southeastern coastal Brazil show generally similar increases in precipitation during the Holocene that also track Southern Hemisphere precessional insolation. Differences between these archives and those from the tropical Andes, however, suggest that precipitation increased to a greater extent at high elevations despite similar forcing mechanisms. The largest increases in tropical Andean SASM rainfall occurred at ~5000, 2200 and 550 yr B.P. The greatest reductions in tropical Andean SASM rainfall occurred between 7000–5000 and 1500–900 yr B.P., latter of which coincided with low lake-levels at Titicaca and desiccation at Laguna Azulcocha. The abrupt transition to wetter Andean conditions at 5000 yr B.P. was synchronous with the reestablishment of the Quelccaya Ice Cap and rising lake levels across the Andes. Further increases in Andean precipitation at 2200 yr B.P. coincided with continued increases in water levels at Titicaca, the onset of varved sedimentation at Pumacocha, and the reestablishment of glaciers in watersheds around Titicaca in the Cordillera Real. The 550 yr B.P. shift marks the onset of the LIA and is concomitant with increased precipitation and glacial advances across the tropical Andes. It is not immediately clear what mechanisms are responsible for the abrupt Holocene shifts in Andean precipitation, particularly the 5000 yr B.P. shift and

subsequent variability increase at 2200 year B.P. It is possible that these transitions are related to non-linear responses of the tropical ocean–atmosphere system to gradual changes in the distribution of insolation on precessional timescales. Possible feedback mechanisms may include the distribution and extent of sea ice in both hemispheres and changes in ENSO. Decadal to multi-century variations in SASM precipitation may also reflect corresponding changes in the latitude of the ITCZ. This idea is consistent with the relationship between SASM intensity and the latitude of the ITCZ during the Holocene and during the last 2000 years (Bird et al., 2011). More work with global climate model simulations is needed, however, to evaluate the relative contributions various forcing mechanisms. Lastly, our results suggest that SASM precipitation over the tropical Andes is more sensitive to long-term and abrupt climate events than Amazon Basin precipitation. This is in agreement with recent model and observational studies and has important implications for the affect of warming trends on Andean water resources.

Supplementary materials related to this article can be found online at doi:10.1016/j.epsl.2011.08.040.

Acknowledgments

Funding for this project was provided by the Earth System History program at the National Science Foundation. We thank Nathan Stansell, Colin Cooke, Jaime Escobar, Eden Diaz, Alijandro Chu, Michael Rosenmeier, James B. Richardson III, Matt Cavallari, and Jeffery Evens for their contributions to this research. The authors further acknowledge the University of Minnesota Limnological Research Center and the facilities, scientific and technical assistance of the Materials Micro-Characterization Laboratory of the Department of Mechanical Engineering and Materials Science, Swanson School of Engineering, University of Pittsburgh. Lastly, we thank Vera Markgraf and one anonymous reviewer for their contribution to the paper.

References

Abbott, M., Wolfe, B.B., Wolfe, A.P., Seltzer, G.O., Aravena, R., Mark, B.G., Polissar, P.J., Rodbell, D.T., Rowe, H.D., Vuille, M., 2003. Holocene paleohydrology and glacial history of the central Andes using multiproxy lake sediment studies. Palaeogeogr. Palaeoclimatol. Palaeoecol. 194, 123–138.

Abbott, M.B., Binford, M.W., Brenner, M., Kelts, K.R., 1997a. A 3500 ^{14}C yr high-resolution record of water-level changes in Lake Titicaca, Bolivia/Peru. Quat. Res. 47, 169–180.

Abbott, M.B., Seltzer, G.O., Kelts, K.R., Southon, J., 1997b. Holocene paleohydrology of the tropical Andes from lake records. Quat. Res. 47, 70–80.

Abbott, M.B., Stafford, T.W., 1996. Radiocarbon geochemistry of modern and ancient Arctic lake systems, Baffin Island, Canada. Quat. Res. 45, 300–311.

Abril, J.M., 2003. Difficulties in interpreting fast mixing in the radiometric dating of sediments using ^{210}Pb and ^{137}Cs. J. Paleolimnol. 30, 407–414.

Appleby, P.G., N., J.P., Gifford, D.W., Godfrey, M.J., Oldfield, F., Anderson, N.J., Battarbee, R.W., 1986. ^{210}Pb dating by low background gamma counting. Hydrobiologia 143, 21–27.

Appleby, P.G., Oldfield, F., 1983. The assessment of ^{210}Pb data from sites with varying sedimentation accumulation rates. Hydrobiologia 103, 29–35.

Baker, P.A., Rigsby, C.A., Seltzer, G.O., Fritz, S.C., Lowenstein, T.K., Bacher, N.P., Veliz, C., 2001a. Tropical climate changes at millennial and orbital timescales on the Bolivian Altiplano. Nature 409, 698–701.

Baker, P.A., Seltzer, G.O., Fritz, S.C., Dunbar, R.B., Grove, M.J., Tapia, P.M., Cross, S.L., Rowe, H.D., Broda, J.P., 2001b. The history of South American tropical precipitation for the past 25,000 years. Science 291, 640–643.

Bird, B.W., Abbott, M.B., Vuille, M., Rodbell, D.T., Stansell, N.D., Rosenmeier, M.F., 2011. A 2300-year-long annually resolved record of the South American summer monsoon from the Peruvian Andes. PNAS 108, 8583–8588.

Bowen, G.J., Wassenaar, L.I., Hobson, K.A., 2005. Global application of stable hydrogen and oxygen isotopes to wildlife forensics. Oecologia 143, 337–348.

Bowen, G.J., Wilkinson, B., 2002. Spatial distribution of δ^1 O in meteoric precipitation. Geology 30, 315–318.

Clement, A.C., Seager, R., Cane, M.A., 2000. Suppression of El Niño during the mid-Holocene by changes in the Earth's orbit. Paleoceanography 15, 731–737.

Cruz, F.W., Vuille, M., Burns, S.J., Wang, X., Cheng, H., Werner, M., Edwards, R.L., Karmann, I., Auler, A.S., Nguyen, a.H., 2009. Orbitally driven east–west antiphasing of South American precipitation. Nat. Geosci. 2, 210–214.

Emile-Geay, J., Cane, M.A., Seager, R., Kaplan, A., Almasi, P., 2007. El Niño as a mediator of the solar influence on climate. Paleoceanography 22, PA3210.

Erten, H.N., Von Gunten, H.R., Sturm, M., 1985. Dating of sediments from Lake Zurich (Switzerland) with ^{210}Pb and ^{137}Cs. Aquat. Sci. Res. Across Boundaries 47, 5–11.

Francus, P., Keimig, F., Besonen, M., 2002. An algorithm to aid varve counting and measurement from thin-sections. J. Paleolimnol. 28, 283–286.

Hardy, D.R., Vuille, M., Braun, C., Keimig, F., Bradley, R.S., 1998. Annual and daily meteorological cycles at high altitude on a tropical mountain. Bull. Am. Meteorol. Soc. 79, 1899–1913.

Hastenrath, S., Polzin, D., Francou, B., 2004. Circulation variability reflected in ice core and lake records of the southern tropical Andes. Clim. Change 64, 361–375.

Hodell, D.A., Kanfoush, S.L., Shemesh, A., Crosta, X., Charles, C.D., Guilderson, T.P., 2001. Abrupt cooling of Antarctic Surface waters and sea ice expansion in the South Atlantic sector of the Southern Ocean at 5000 cal yr B.P. Quat. Res. 56, 191–198.

Hoffmann, G., Ramirez, E., Taupin, J.D., Francou, B., Ribstein, P., Delmas, R.J., Durr, H., Gallaire, R., Simoes, J., Schotterer, U., Stievenard, M., Werner, M., 2003. Coherent isotope history of Andean ice cores over the last century. Geophys. Res. Lett. 30, 1179–1182.

Jones, P.D., Mann, M.E., 2004. Climate over past millennia. Rev. Geophys. 42.

Kim, S.-T., O'Neil, J.R., 1997. Equilibrium and nonequilibrium oxygen isotope effects in synthetic carbonates. Geochim. Cosmochim. Acta 61, 3461–3475.

Lewis, S.L., Brando, P.M., Phillips, O.L., Heijden, G.M.F.v.d., Nepstad, D., 2011. The 2010 Amazon drought. Science 331, 554.

Li, H.-C., Ku, T.-L., 1997. δ^{13}C–δ^{18}O covariance as a paleohydrological indicator for closed-basin lakes. Palaeogeogr. Palaeoclimatol. Palaeoecol. 133, 69–80.

Liu, Z., Otto-Bliesner, B.L., Kutzbach, J., Li, L., Shields, C., 2003. Coupled climate simulation of the evolution of global monsoons in the Holocene. J. Clim. 16, 2472–2490.

Moberg, A., Sonechkin, D.M., Holmgren, K., Datsenko, N.M., Karlen, W., 2005. Highly variable Northern Hemisphere temperatures reconstructed from low- and high-resolution proxy data. Nature 433, 613–617.

O'Neil, J.R., Clayton, R.N., Mayeda, T.K., 1969. Oxygen isotope fractionation in divalent metal carbonates. J. Chem. Phys. 51, 5547.

Polissar, P.J., Abbott, M.B., Shemesh, A., Wolfe, A.P., Bradley, R.S., 2006a. Holocene hydrologic balance of tropical South America from oxygen isotopes of lake sediment opal, Venezuelan Andes. Earth Planet. Sci. Lett. 242, 375–389.

Polissar, P.J., Abbott, M.B., Wolfe, A.P., Bezada, M., Rull, V., Bradley, R.S., 2006b. Solar modulation of Little Ice Age climate in the tropical Andes. PNAS 103, 8937–8942.

Quispensivana, L.Q., 1996. Mapa geologico del cuadrangulo de Cerro de Pasco. Ministerio de Energia y Minas, Instituto Geologico Minero y Metalurigico.

Rabatel, A., Francou, B., Jomelli, V., Naveau, P., Grancher, D., 2008. A chronology of the Little Ice Age in the tropical Andes of Bolivia (16°S) and its implications for climate reconstruction. Quat. Res. 70, 198–212.

Rabatel, A., Jomelli, V., Naveau, P., Francou, B., Grancher, D., 2005. Dating of Little Ice Age glacier fluctuations in the tropical Andes: Charquini glaciers, Bolivia, 16°S. Comptes Rendus Geosciences, pp. 1311–1322.

Reuter, J., Stott, L., Khider, D., Sinha, A., Cheng, H., Edwards, R.L., 2009. A new perspective on the hydroclimate variability in northern South America during the Little Ice Age. Geophys. Res. Lett. 36, L21706.

Rodbell, D.T., Seltzer, G.O., Mark, B.G., Smith, J.A.S., Abbott, M.B., 2008. Clastic sediment flux to tropical Andean lakes: records of glaciation and soil erosion. Quat. Sci. Rev. 27, 1612–1625.

Row, H.D., Guilderson, T.P., Dunbar, R.B., Southon, J.R., Seltzer, G.O., Mucciarone, D.A., Fritz, S.C., Baker, P.A., 2003. Late Quaternary lake-level changes constrained by radiocarbon and stable isotope studies on sediment cores from Lake Titicaca, South America. Global Planet. Change 38, 273–290.

Rozanski, K., Araguás-Araguás, Gonfiantini, R., 1992. Relation between long-term trends of oxygen-18 isotope composition of precipitation and climate. Science 258, 981–985.

Rozanski, K., Araguas-Araguas, L., Conginatine, R., 1993. Isotopic patterns in modern global precipitation. Climate Change in Continental isotopic Records: Geophys. Monogr. , pp. 1–36.

Schelske, C.L., Peplow, A., Brenner, M., Spencer, C.N., 1994. Low-background gamma counting: applications for ^{210}Pb dating of sediments. J. Paleolimnol. 10, 115–128.

Schmidt, G., LeGrande, A., Hoffmann, G., 2007. Water isotope expressions of intrinsic and forced variability in a coupled ocean–atmosphere model. J. Geophys. Res. 112, D10103.

Seltzer, G., Rodbell, D., Burns, S., 2000. Isotopic evidence for late Quaternary climatic change in tropical South America. Geology 28, 35–38.

Seltzer, G.O., Baker, P.A., Cross, S.L., Dunbar, R.B., Fritz, S., 1998. High-resolution seismic reflection profiles from Lake Titicaca, Peru–Bolivia: evidence for Holocene aridity in the tropical Andes. Geology 26, 167–170.

Solomina, O., Jomelli, V., Kaser, G., Ames, A., Berger, B., Pouyaud, B., 2007. Lichenometry in the Cordillera Blanca, Peru: "Little Ice Age" moraine chronology. Global Planet. Change 59, 225–235.

Stuiver, M., Reimer, P.J., 1993. Extended ^{1} C database and revised CALIB radiocarbon calibration program. Radiocarbon 35, 215–230.

Sturm, C., Hoffmann, G., Langmann, B., 2007. Simulation of the stable water isotopes in precipitation over South America: comparing regional to global circulation models. J. Clim. 20, 3730–3750.

Thompson, L.G., Mosley-Thompson, E., Brecher, H., Davis, M., 2006. Abrupt tropical climate change: past and present. PNAS 103, 10536–10543.

Thompson, L.G., Mosley-Thompson, E., Henderson, K.A., 2000. Ice-core palaeoclimate records in tropical South America since the last Glacial Maximum. J. Quat. Sci. 15, 377–394.

Thompson, L.G., Thompson, E.M., Dansgaard, W., Groots, P.M., 1986. The Little Ice Age as recorded in the stratigraphy of the tropical Quelccaya Ice Cap. Science 234, 361–364.

van Breukelen, M.R., Vonhof, H.B., Hellstrom, J.C., 2008. Fossil dripwater in stalagmites reveals Holocene temperature and rainfall variation in Amazonia. Earth Planet. Sci. Lett. 242, 375–389.

von Gunten, L., Grosjean, M., Rein, B., Urrutia, R., Appleby, P., 2009. A quantitative high-resolution summer temperature reconstruction based on sedimentary pigments from Laguna Aculeo, central Chile, back to AD 850. Holocene 19, 873–881.

Vuille, M., Bradley, R.S., Werner, M., Healy, R., Keimig, F., 2003a. Modeling δ^{1} O in precipitation over the tropical Americas: 1. Interannual variability and climatic controls. J. Geophys. Res. 108, 4174.

Vuille, M., Bradley, R.S., Werner, M., Healy, R., Keimig, F., 2003b. Modeling δ^{1} O in precipitation over the tropical Americas: 2. Simulation of the stable isotope signal in Andean ice cores. J. Geophys. Res. 108, 4175.

Vuille, M., Werner, M., 2005. Stable isotopes in precipitation recording South American summer monsoon and ENSO variability: observations and model results. Clim. Dyn. 25, 401–413.

Wang, X., Auler, A., Edwards, R., Cheng, H., Ito, E., Wang, Y., Kong, X., Solheid, M., 2007. Millennial-scale precipitation changes in southern Brazil over the past 90,000 years. Geophys. Res. Lett. 34, L23701.